Yu Lie
Xi' an Jiaotong University
P. R. China

R. B. Bhat
Concordia University
Canada

Coupled Dynamics of a Rotor-Journal Bearing System Equipped with Thrust Bearings

The rotordynamic coefficients of fixed-pad thrust bearing are introduced and calculated by using the out-domain method, and a general analysis method is developed to investigate the coupled dynamics of a rotor equipped with journal and thrust bearings simultaneously. Considerations include the effects of static tilt parameters of the rotor on rotordynamic coefficients of thrust bearing and the action of thrust bearing on system dynamics. It is shown that thrust bearing changes the load distribution of journal bearings and the static deflection of the rotor and delays the instability of the system considerably in lateral shaft vibration. © *1995 John Wiley & Sons, Inc.*

INTRODUCTION

Hydrodynamic thrust bearings are used in rotating machinery not only to support the axial load, but also to suppress various forces acting in the axial direction. As these exciting forces have increased in recent years, prediction of the static and dynamic characteristics of hydrodynamic thrust bearing is becoming more and more important. Knowledge of exact performance of hydrodynamic thrust bearings applicable to practical design is still limited at present.

Literature dealing with the static performance of thrust bearing can be found in Etsion (1978) and in Jeng and Szeri (1986). A few studies that described the rotordynamic coefficients of thrust bearing have been reported in Someya and Fukuda (1972) and in Zhu Qin et al. (1990). It must be noted that in the above research, effects of the static tilt of the runner are not considered in all the studies and those methods in the above mentioned articles cannot be used to investigate the interaction relationship between the static tilt of the runner and the thrust bearing performance. In the pioneering research of Mittwollen et al. (1990), a series of rotordynamic coefficients of thrust bearing are defined and used for the investigation of the action of thrust bearing upon the lateral vibration in a rotor system. However, in their research the static tilt of the runner is also neglected.

The present article focusses on the analysis of the effects of static tilt of the runner on bearing performance and the discussion of coupled dynamics of a rotor system equipped with journal and thrust bearings.

Although there exist various numerical methods to solve two dimensional lubrication problems, the boundary element method (BEM) has an advantage due to the reduction of freedom and is widely adopted in engineering. However, this method has a serious disadvantage in that

Received July 5, 1993; Accepted July 12, 1994.

Shock and Vibration, Vol. 2, No. 1, pp. 1–14 (1995)

CCC 1070-9622/95/02001-14

the singularity of the fundamental solution is taken on the boundary of the problem domain, which requires the evaluation of a series of singular integrals that incur a sizable computational overhead. In the present work, the out-domain method, which is a modified method described by Trefftz (1926) and Patterson and Sheikh (1982), is used to solve the Reynolds equation in order to avoid the singularity in the integrals. Another purpose of the present research is the investigation on system dynamics.

When a rotor is supported by journal bearings in a radial direction and thrust bearings in an axial direction, thrust bearings play a significant role on system behavior as important as that of journal bearings. They provide oil film forces and moments to the rotor, stiffen or relax the rotor, change both static and dynamic boundary conditions of system, and also change the critical speed of the rotor and system stability.

The interactions among the rotor, the journal, and thrust bearings are quite complex. While considering the rotor, the journal bearings, and the thrust bearings as a whole system, determination of the performance of thrust bearing requires a priori knowledge of the motion of the rotor.

In the static equilibrium state, existence of thrust bearings renders the solution for the load distribution statically indeterminate. In the dynamic state, although dynamic behavior of thrust bearings can be described by a series of rotordynamic coefficients, these coefficients depend strongly on tilt parameters of the rotor and must be precalculated. Simultaneously, the coupling action of the thrust bearings on the system makes it necessary that an effective numerical and iterative method is found in order to predict system behavior.

Based on the above mentioned principle, this article presents a general analysis method in which the coupling actions among the rotor, the journal bearings, and the thrust bearings are duly taken into account. As an example of the application of this method, static and dynamic behavior of a rotor equipped with journal and thrust bearings are calculated and discussed in detail.

TILT PARAMETERS OF RUNNER

A sketch of a flat sector pad thrust bearing in operation is shown in Fig. 1a. The motion of the runner can be described by its translational velocities $\dot{x}$, $\dot{y}$, and $\dot{z}$ and rotating angular speeds ω, $\dot{\varphi}$, and $\dot{\psi}$ by taking (x, y, z) as the principal coordinate system. The origin of the coordinate system (x, y, z) coincides with the center of the runner, and the axis z coincides with the rotor center line. ψ is defined to be the angle, measured in the yz plane, by which axis z leads axis z_1 and axis y leads axis y_1. Similarly φ is measured in the xz_1 plane by which axis z_1 leads axis z_2 and axis x leads axis x_2 [Fig. 1(b)].

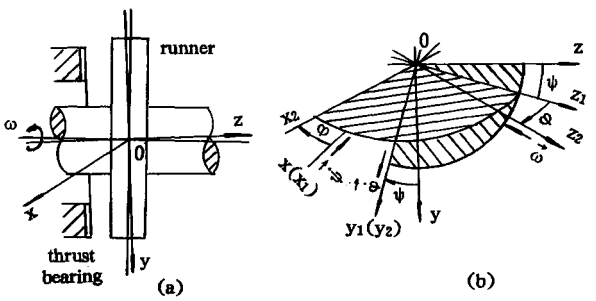

FIGURE 1 (a) Thrust bearing in operation and (b) motion of the runner.

ROTORDYNAMIC COEFFICIENTS OF THRUST BEARING

Although the Reynold's equation has its generalized form,

$$\frac{\partial}{\partial y}\left(\frac{h^3}{12\mu}\frac{\partial p}{\partial y}\right) + \frac{\partial}{\partial x}\left(\frac{h^3}{12\mu}\frac{\partial p}{\partial x}\right) = \frac{\omega}{2}\frac{\partial h}{\partial \theta} + \frac{\partial h}{\partial t} \quad (1)$$

where p is the oil film pressure, h the oil film thickness, μ the dynamic lubricant viscosity, ω the shaft angular speed, t the time, and x, y, and θ are the coordinates shown in Fig. 2.

The oil film thickness h now is not only the function of pad parameters, but also the function of tilt parameters φ and ψ, and h varies in both radial and circumferential directions. Tilting angles φ and ψ, which may result from shaft deformation or from misalignment of the rotor, changes the oil film thickness, the moment due to oil film forces, and the boundary conditions of the system. Usually the oil film thickness at any arbitrary point (r, θ) in a local coordinate system $o - x_k y_k z_k$ can be expressed as follows (Fig. 2):

$$h(r, \theta) = z_0 + \alpha_0 r \sin(\theta_p - \theta) - \psi_k r \cos\theta - \varphi_k r \sin\theta \quad (2)$$

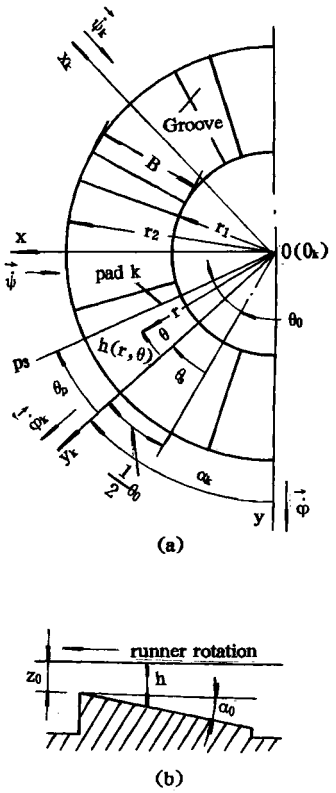

FIGURE 2 (a) Thrust bearing and (b) oil film thickness.

where z_0 is the oil film thickness at the position of pitch line op_3, α_0 the pad parameter, θ_p the angular coordinate of pitch line op_3, r_1 and r_2 the inner and outer radii, B the width of thrust pad, θ_0 the angular extent of pad, r and θ the radial and angular coordinates. φ_k and ψ_k represent the tilt parameters for the kth pad in the local coordinate system $o - x_k y_k z_k$, which can be obtained by a rotation of the principal coordinate system $o - xyz$, and α_k is the rotating angle of the coordinate system. For a thrust bearing consisting of multiple pads, calculation for each pad can be performed in its local coordinate system. When the rotor has tilting angles named φ and ψ in the principal coordinate system, tilt parameters φ_k and ψ_k for the kth pad in the $o - x_k y_k z_k$ system can be found by using the following equation:

$$\begin{vmatrix} \varphi_k \\ \psi_k \end{vmatrix} = \begin{vmatrix} \cos\alpha_k & -\sin\alpha_k \\ \sin\alpha_k & \cos\alpha_k \end{vmatrix} \begin{vmatrix} \varphi \\ \psi \end{vmatrix}. \tag{3}$$

Let $r = B\bar{r}$, $x = B\bar{x}$, $y = B\bar{y}$, $z_0 = h_e\bar{z}_0$, $h = h_e\bar{h}$, $\mu = \mu_0\bar{\mu}$, $\rho = \rho_0\bar{\rho}$, $p = (\mu_0\omega B^2/h_e^2)\,P$, $t = (1/\omega)\,T$, $\varphi = (h_e/B)\,\bar{\varphi}$, $\psi = (h_e/B)\,\bar{\psi}$, $\varphi_k = (h_e/B)\,\bar{\varphi}_k$, $\psi_k = (h_e/B)\,\bar{\psi}_k$. h_e, μ_o, and ρ_o are the reference film thickness, lubricant viscosity, and lubricant density, respectively. Introducing two new variables a and U into Eq. (1) and dimensionalizing Eq. (1) yields

$$\begin{aligned} &\nabla^2 U_s = f_s + g_s U_s \\ &(\text{for } s = 0, z, \varphi, \psi, z', \varphi', \psi') \end{aligned} \tag{4}$$

with the operator

$$\nabla^2 = \frac{\partial}{\partial \bar{x}^2} + \frac{\partial}{\partial \bar{y}^2}$$

$$U_s = a^{3/2}\bar{P}_s + \frac{3}{2}a^{1/2}a_s\bar{P}_0$$

$$a = \bar{\mu}^{-1/3}\bar{h}; \quad U_0 = a^{3/2}\bar{P}_0; \quad a_s = \frac{\partial a}{\partial s}.$$

In the above expressions, the subscript s stands for the small perturbation about the equilibrium position of the runner. When $s = 0$, Eq. (4) describes the static pressure distribution U_0. For $s = z, \varphi, \cdots, \varphi'$, and ψ', variables U_z, U_φ, ..., $U_{\varphi'}$, and $U_{\psi'}$, stand for the derivatives of U with respect to perturbations z, φ, ..., φ', and ψ'. The superscript "$-$" represents the dimensionless variable, and "," stands for the derivation with respect to T.

The boundary conditions for Eq. (4) give

$$U_0|_\Gamma = \bar{h}^{3/2}\bar{P}_0|_\Gamma \quad (\text{for } s = 0)$$

or

$$U_s|_\Gamma = \frac{3}{2}\bar{h}^{1/2}\frac{\partial \bar{h}}{\partial s}\bar{P}_0|_\Gamma \quad (\text{for } s = z, \varphi, \psi, z', \varphi', \psi'). \tag{5}$$

The coefficients f_s and g_s are listed in Appendix A.

Static Performance: Single Pad

The load capacity of a single pad in the local coordinate system $o - x_k y_k z_k$ gives

$$\vec{W}_0 = W_{xo}\vec{i} + W_{yo}\vec{j} + W_{zo}\vec{k} \tag{6}$$

with the components

$$\begin{vmatrix} W_{xo} \\ W_{yo} \\ W_{zo} \end{vmatrix} = W_0 \begin{vmatrix} \sin\varphi_k \\ \cos\varphi_k \sin\psi_k \\ \cos\varphi_k \cos\psi_k \end{vmatrix} = W_0 \begin{vmatrix} \varphi_k \\ \psi_k \\ 1.0 \end{vmatrix} \tag{7}$$

where

$$W_0 = \int \int_\Omega p_0 r dr d\theta. \tag{8}$$

Besides W_0, what we pay more attention to is the moment due to the normal pressure p_0,

$$\vec{M}_0^p = M_{x0}^p \vec{i} + M_{y0}^p \vec{j} + M_{z0}^p \vec{k} \tag{9}$$

with

$$\begin{vmatrix} M_{x0}^p \\ M_{y0}^p \\ M_{z0}^p \end{vmatrix} = \begin{vmatrix} \int \int_\Omega p_0 r^2 \cos\theta \, dr \, d\theta \\ -\int \int_\Omega p_0 r^2 \sin\theta \, dr \, d\theta \\ -M_{xo}^p \varphi_k - M_{yo}^p \psi_k \end{vmatrix} \tag{10}$$

Rotordynamic Coefficients: Single Pad

The increment of $\vec{W}$ in the case of small perturbation can be expressed by linear force stiffness and damping coefficients

$$\Delta \vec{W} = \Delta W_x \vec{i} + \Delta W_y \vec{j} + \Delta W_z \vec{k} \tag{11}$$

with

$$\begin{vmatrix} \Delta W_x \\ \Delta W_y \\ \Delta W_z \end{vmatrix} = \begin{vmatrix} k_{xz}^w & k_{x\varphi}^w & k_{x\psi}^w \\ k_{yz}^w & k_{y\varphi}^w & k_{y\psi}^w \\ k_{zz}^w & k_{z\varphi}^w & k_{z\psi}^w \end{vmatrix}_k \begin{vmatrix} \Delta z \\ \Delta \varphi \\ \Delta \psi \end{vmatrix}_k + \begin{vmatrix} d_{xz}^w & d_{x\varphi}^w & d_{x\psi}^w \\ d_{yz}^w & d_{y\varphi}^w & d_{y\psi}^w \\ d_{zz}^w & d_{z\varphi}^w & d_{z\psi}^w \end{vmatrix} \begin{vmatrix} z' \\ \varphi' \\ \psi' \end{vmatrix}. \tag{12}$$

Similarly introducing the moment stiffness and damping coefficients yields the increment of the moment due to normal pressure.

$$\Delta \vec{M}^p = \Delta M_x^p \vec{i} + \Delta M_y^p \vec{j} + \Delta M_z^p \vec{k} \tag{13}$$

with

$$\begin{vmatrix} \Delta M_x^p \\ \Delta M_y^p \\ \Delta M_z^p \end{vmatrix} = \begin{vmatrix} k_{xz}^m & k_{x\varphi}^m & k_{x\psi}^m \\ k_{yz}^m & k_{y\varphi}^m & k_{y\psi}^m \\ k_{zz}^m & k_{z\varphi}^m & k_{z\psi}^m \end{vmatrix}_k \begin{vmatrix} \Delta z \\ \Delta \varphi \\ \Delta \psi \end{vmatrix}_k + \begin{vmatrix} d_{xz}^m & d_{x\varphi}^m & d_{x\psi}^m \\ d_{yz}^m & d_{y\varphi}^m & d_{y\psi}^m \\ d_{zz}^m & d_{z\varphi}^m & d_{z\psi}^m \end{vmatrix} \begin{vmatrix} z' \\ \varphi' \\ \psi' \end{vmatrix}_k. \tag{14}$$

In Eq. (12), k_{is}^w is defined as the force stiffness coefficients in the i direction, corresponding to the displacement or the angular displacement perturbation s; d_{is}^w is the force damping coefficients, corresponding to the velocity perturbation s', k_{is}^m the moment stiffness coefficients, and d_{is}^m the moment damping coefficients ($i = x, y, z$; $s = z, \varphi, \psi$). Formulas of k_{is}^w, d_{is}^w, k_{is}^m, and d_{is}^m are listed in Appendix B.

Static and Dynamic Characteristics of Multipad Thrust Bearing

For a thrust bearing consisting of multiple pads, calculation for each pad can be performed in its local coordinate system for the sake of simplicity, and then these characteristics calculated can be transformed into the principal system by using the following formulas. For the force and moment components,

$$\{W\}_k = [A_1]_k \{\widetilde{W}\}_k \tag{15}$$

$$\{M^p\}_k = [A_1]_k \{\widetilde{M}^p\}_k \tag{16}$$

For the force stiffness and damping coefficients,

$$\begin{aligned} \{K_z^w\}_k &= [A_2]_k \{\widetilde{K}_z^w\}_k; \quad \{D_z^w\}_k = [A_2]_k \{\widetilde{D}_z^w\}_k \\ \{K_{xy}^w\}_k &= [A_3]_k \{\widetilde{K}_{xy}^w\}_k; \quad \{D_{xy}^w\}_k = [A_3]_k \{\widetilde{D}_{xy}^w\}_k. \end{aligned} \tag{17}$$

For the moment stiffness and damping coefficients,

$$\begin{aligned} \{K_z^m\}_k &= [A_2]_k \{\widetilde{K}_z^m\}_k; \quad \{D_z^m\}_k = [A_2]_k \{\widetilde{D}_z^m\}_k \\ \{K_{xy}^m\}_k &= [A_3]_k \{\widetilde{K}_{xy}^m\}_k; \quad \{D_{xy}^m\}_k = [A_3]_k \{\widetilde{D}_{xy}^m\}_k. \end{aligned} \tag{18}$$

In the above equations, vectors $\{W\}_k = (W_{xo}, W_{yo}, W_{zo})_k^T$, $\{M^p\}_k = (M_{xo}^p, M_{yo}^p, M_{zo}^p)_k^T$, $\{K_z^w\}_k = (k_{zz}^w, k_{z\varphi}^w, k_{z\psi}^w)_k^T$, $\{D_z^w\}_k = (d_{zz}^w, d_{z\varphi}^w, d_{z\psi}^w)_k^T$, $\{K_{xy}^w\}_k = (k_{xz}^w, k_{x\varphi}^w, k_{x\psi}^w, k_{yz}^w, k_{y\varphi}^w, k_{y\psi}^w)_k^T$, $\{D_{xy}^w\}_k = (d_{xz}^w, d_{x\varphi}^w, d_{x\psi}^w, d_{yz}^w, d_{y\varphi}^w, d_{y\psi}^w)_k^T$, $\{K_z^m\}_k = (k_{zz}^m, k_{z\varphi}^m, k_{z\psi}^m)_k^T$, $\{D_z^m\}_k = (d_{zz}^m, d_{z\varphi}^m, d_{z\psi}^m)_k^T$, $\{K_{xy}^m\}_k = (k_{xz}^m, k_{x\varphi}^m, k_{x\psi}^m, k_{yz}^m, k_{z\varphi}^m, k_{z\psi}^m)_k^T$, $\{D_{xy}^m\}_k = (d_{xz}^m, d_{x\varphi}^m, d_{x\psi}^m, d_{yz}^m, d_{y\varphi}^m, d_{y\psi}^m)_k^T$, and the transfer matrixes

$$[A_1]_k = \begin{vmatrix} \cos a_k & \sin a_k & 0 \\ -\sin a_k & \cos a_k & 0 \\ 0 & 0 & 1 \end{vmatrix} \quad [A_2]_k = \begin{vmatrix} 1 & 0 & 0 \\ 0 & \cos a_k & \sin a_k \\ 0 & -\sin a_k & \cos a_k \end{vmatrix}$$

$$[A_3]_k = \begin{vmatrix} \cos a_k & 0 & 0 & \sin a_k & 0 & 0 \\ 0 & \cos^2 a_k & (\sin a_k \cos a_k) & 0 & (\sin a_k \cos a_k) & \sin^2 a_k \\ 0 & (-\sin a_k \cos a_k) & \cos^2 a_k & 0 & (-\sin^2 a_k) & (\sin a_k \cos a_k) \\ -\sin a_k & 0 & 0 & \cos a_k & 0 & 0 \\ 0 & (-\sin a_k \cos a_k) & -\sin^2 a_k & 0 & \cos^2 a_k & (\sin a_k \cos a_k) \\ 0 & \sin^2 a_k & (-\sin a_k \cos a_k) & 0 & (\sin a_k \cos a_k) & \cos^2 a_k \end{vmatrix} \tag{19}$$

It must be pointed out that for a multipad thrust bearing, it is difficult to calculate so many coefficients for all the pads one by one. In fact, this principle provides a new method that can be used to accelerate the calculation procedure. When all the pads have the same pad parameters except the tilt parameters of the runner, only a single pad needs to be calculated with a range of tilt parameters in the local coordinate system. Now the problem is to find a way of using the known data sufficiently for the calculation of pads. For certain tilt parameters φ_0 and ψ_0 of the runner, φ_k and ψ_k for the kth pad can be found by using Eq. (3). Because the only difference among all the pads, from the point of the local coordinate system, is φ_k and ψ_k, the known data mentioned above now can be used to find all the static and dynamic characteristics by using the curve-fitting method according to φ_k and ψ_k. Furthermore, formulas (15)–(19) can be used to transfer these data into the principal coordinate system, then the static characteristics and rotordynamic coefficients for the whole bearing can be obtained by simply putting those quantities for each pad together.

OUT-DOMAIN METHOD BY FUNDAMENTAL SOLUTION

In order to avoid the integral singularity along the boundary, this article uses the out-domain method to solve Eq. (4). Similar to the indirect BEM, it is necessary to use the fundamental solution for the general solution of Eq. (4).

$$u^* = \ln \frac{1}{r(p, Q)} \tag{20}$$

where p is the point under consideration, Q is the source point, and $r(p, Q)$ is the displacement between p and Q.

The special solution of Eq. (4) can be written as

$$u_q = \int\int_\Omega -\frac{1}{2\pi} (f_s + g_s U_s) u^* \, d\Omega(q). \tag{21}$$

Assuming that there exists a source field with a density function $-(1/2\pi)(f_s + g_s U_s)$ overall the domain Ω, Eq. (21) represents the contribution of the whole field to a certain point p. The difference between the BEM and the present method lies in that in the BEM, no matter whether the direct or indirect BEM is adopted, the linear integral is always performed along the real boundary Γ of the domain considered. In the present research, the source function $\omega(Q)$ is distributed not along the real boundary Γ but along an auxiliary boundary Γ^*, which involves the domain Ω considered (Fig. 3).

The solution of Eq. (4) is considered to be the superposition of the common action of the real field with the density function $-(1/2\pi)(f_s + g_s U_s)$ and the imaginary field with the density function $\omega(Q)$ to be determined. For each point p (including the point on the boundary Γ),

$$U_s(P) = \int_{\Gamma^*} \omega(Q) u^*(p_i, Q) d\Gamma(Q) + \int\int_\Omega -\frac{1}{2\pi} (f_s + g_s U_s) u^* d\Omega. \tag{22}$$

In Eq. (22), the linear integral is only along the auxiliary boundary Γ^*. It follows that the displacement $r(p, Q)$ is not always equal to zero, so the singularity of the linear integral can be avoided, which follows an obvious computational advantage over the BEM in that it requires

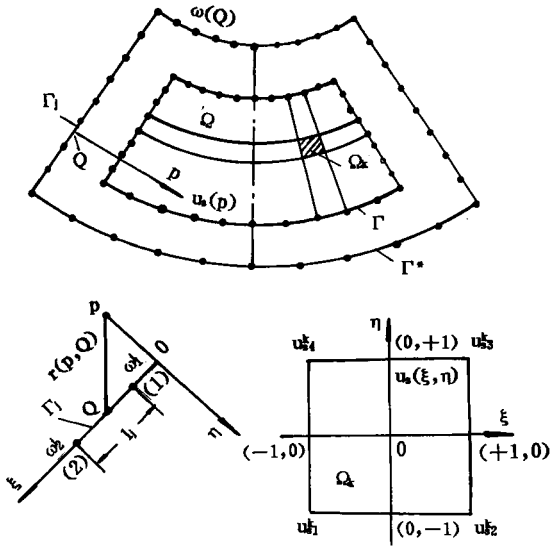

FIGURE 3 The out-domain method by using fundamental solution.

much less effort to set up the system equations, and the singular quantities need not be handled.

Choice of function $\omega(Q)$ must satisfy the necessary boundary conditions on boundary Γ. Numerical implement is the same as that in the BEM. When the auxiliary boundary Γ^* is divided into M boundary elements and the domain Ω is divided into S quadrilateral elements, the discretized form of Eq. (22) gives

$$U_s(p_i) = \sum_{j=1}^{M} \int_{\Gamma_j^*} \omega(Q) u^*(p_i, Q)\, d\Gamma(Q) + \sum_{k=1}^{S} \int\int_{\Omega_k} -\frac{1}{2\pi} u^*(p_i, q)(f_s(q) + g_s(q)U_s(q))\, d\Omega. \quad (23)$$

By introducing the shape functions n_l for the linear element ($l = 1, 2$) and m_r for the quadrilateral element ($r = 1, 2, 3, 4$), Eq. (22) can be rewritten as

$$U_s(p_i) = \sum_{j=1}^{M} \left\{ \sum_{l=1}^{2} b_l^j \omega_l^j \right\} + \sum_{k=1}^{S} \left\{ \sum_{r=1}^{4} c_r^k f_{sr}^k \right\} + \sum_{k=1}^{S} \left\{ \sum_{r=1}^{4} c_r^k g_{ur}^k \right\} \quad (24)$$

with coefficients

$$b_l^j = \int_{\Gamma_j^*} n_l u^*(p_i, Q)\, d\Gamma(Q)$$
$$c_r^k = \int\int_{\Omega_k} -\frac{1}{2\pi} m_r u^*(p_i, q)\, d\Omega(q) \quad (25)$$

where ω_l^j represents the value of density of the lth local node at the jth boundary element, f_{sr}^k the value of $f_s(q)$ at the rth local node on the kth quadrilateral element, and g_{ur}^k the value of $g_s(q)U_s(q)$ at the rth local node on quadrilateral element k, respectively. The shape functions

$$n_1 = \frac{1}{l_j}(\xi_2 - \xi)$$
$$n_2 = \frac{1}{l_j}(\xi - \xi_1) \quad (26a)$$

$$m_1 = \frac{1}{4}(1 - \xi)(1 - \eta)$$
$$m_2 = \frac{1}{4}(1 + \xi)(1 - \eta)$$
$$m_3 = \frac{1}{4}(1 + \xi)(1 + \eta) \quad (26b)$$
$$m_4 = \frac{1}{4}(1 - \xi)(1 + \eta).$$

Applying Eq. (24) to all inner nodes and boundary nodes, we obtain the system equation in matrix form:

$$\begin{aligned}\{U\}_{N\times 1} &= \{B\}_{N\times N_b}\{\omega\}_{N_b\times 1} + \{C\}_{N\times N}\{F\}_{N\times 1} \\ &\quad + \{C\}_{N\times N}\{G\}_{N\times N}\{U\}_{N\times 1} \\ &= \{B\}_{N\times N_b}\{\omega\}_{N_b\times 1} + \{CF\}_{N\times 1} \\ &\quad + \{D\}_{N\times N}\{U\}_{N\times 1}\end{aligned} \quad (27)$$

where coefficients matrices $\{B\}$ and $\{C\}$ are formed by Eqs. (25) and (26), vector $\{F\}$ consists of the values of $f_s(q)$ at each node, matrix $\{G\}$ is a diagonal matrix with the diagonal elements g_{s1}, $g_{s2}, \ldots, g_{sN}$.

Vector $\{\omega\}$ is determined by the boundary condition (5). Taking the first boundary value problem as an example, let $\{U_1\}$ represent the values known on boundary Γ and $\{U_2\}$ the unknowns to be found. Reordering Eq. (27), we obtain

$$\begin{Bmatrix} U_1 \\ U_2 \end{Bmatrix} = \begin{bmatrix} B^1 \\ B_2 \end{bmatrix} [\omega] + \begin{Bmatrix} CF_1 \\ CF_2 \end{Bmatrix} + \begin{bmatrix} D_{11} & D_{12} \\ D_{21} & D_{22} \end{bmatrix} \begin{Bmatrix} U_1 \\ U_2 \end{Bmatrix}, \quad (28)$$

The density distribution $\{\omega\}$ can be solved by the following equation:

$$\{\omega\} = [B_1 + D_{12}(I - D_{22})^{-1}B_2]^{-1}\{[I - D_{11} - D_{12}(I - D_{22})^{-1}D_{21}]U_1 - [CF_1] - D_{12}(I - D_{22})^{-1}CF_2\} \tag{29}$$

when $\{\omega\}$ is found, $\{U_2\}$ can be solved by using Eq. (30):

$$\{U_2\} = (I - D_{22})^{-1}B_2\{\omega\} + (I - D_{22})^{-1}\{CF_2\} + (I - D_{22})^{-1}D_{21}\{U_1\}. \tag{30}$$

The Neuman problem of the mixed boundary value problem can be handled in a similar manner.

COUPLED DYNAMICS OF A ROTOR SYSTEM EQUIPPED WITH JOURNAL AND THRUST BEARINGS

Equilibrium Equation of Rotor Shaft

When the rotor is divided into n elements by using the method in Myklestad (1944), the equation for the kth shaft element in the xz plane is written as (Fig. 4)

$$\begin{vmatrix} x \\ \varphi \\ M \\ S \end{vmatrix}_k^r = \begin{vmatrix} 1 & l & \frac{l^2}{2EI} & -\frac{l^3}{6EI} \\ 0 & 1 & \frac{l}{EI} & -\frac{l^2}{2EI} \\ 0 & 0 & 1 & -l \\ 0 & 0 & 0 & 1 \end{vmatrix}_k \begin{vmatrix} x \\ \varphi \\ M \\ S \end{vmatrix}_{k-1}^r + \begin{vmatrix} 0 \\ 0 \\ \Sigma M \\ \Sigma F_x \end{vmatrix}_k \tag{31}$$

and in the yz plane

$$\begin{vmatrix} y \\ \psi \\ N \\ Q \end{vmatrix}_k^r = \begin{vmatrix} 1 & l & \frac{l^2}{2EI} & -\frac{l^3}{6EI} \\ 0 & l & \frac{l}{EI} & -\frac{l^2}{2EI} \\ 0 & 0 & 1 & -l \\ 0 & 0 & 0 & 1 \end{vmatrix}_k \begin{vmatrix} y \\ \psi \\ N \\ Q \end{vmatrix}_{k-1}^r + \begin{vmatrix} 0 \\ 0 \\ \Sigma N \\ \Sigma F_y \end{vmatrix}_k \tag{32}$$

where x, y are the displacements, φ and ψ the tilting angles of shaft, M and N the moments in xz and yz planes, S and Q the shear stresses, l the length of shaft element, E the modulus of elasticity, and I the inertia moment. ΣM and ΣN represent the external moments acting on xz and yz planes, respectively, that result from the gyroscopic moments and the moments due to thrust bearing acting on mass point k. ΣF_x and ΣF_y are external forces in x and y directions.

Static Balance and Load Distribution in Journal Bearings

Because of the effects of thrust bearing on rotor behavior, the solution of the load distribution in journal bearings becomes a statically indeterminate problem even in simple cases. Under static balance conditions, the load distribution can be found by using Eqs. (31) and (32) expressed as

$$\begin{vmatrix} x \\ \varphi \\ M \\ S \end{vmatrix}_k^r = \begin{vmatrix} 1 & l & \frac{l^2}{2EI} & -\frac{l^3}{6EI} \\ 0 & 1 & \frac{l}{EI} & -\frac{l^2}{2EI} \\ 0 & 0 & 1 & -l \\ 0 & 0 & 0 & 1 \end{vmatrix}_k \begin{vmatrix} x \\ \varphi \\ M \\ S \end{vmatrix}_{k-1}^r + \begin{vmatrix} 0 \\ 0 \\ -M_{y0}^p \\ F_{x0}^j - W_{x0} \end{vmatrix}_k \tag{33}$$

$$\begin{vmatrix} y \\ \psi \\ N \\ Q \end{vmatrix}_k^r = \begin{vmatrix} 1 & l & \frac{l^2}{2EI} & -\frac{l^3}{6EI} \\ 0 & 1 & \frac{l}{EI} & -\frac{l^2}{2EI} \\ 0 & 0 & 1 & -l \\ 0 & 0 & 0 & 1 \end{vmatrix}_k \begin{vmatrix} y \\ \psi \\ N \\ Q \end{vmatrix}_{k-1}^r + \begin{vmatrix} 0 \\ 0 \\ M_{x0}^p \\ F_{y0}^j - P_g - W_{y0} \end{vmatrix}_k \tag{34}$$

where M_{x0}^p and M_{y0}^p represent the moment components of thrust bearing in xz and yz planes,

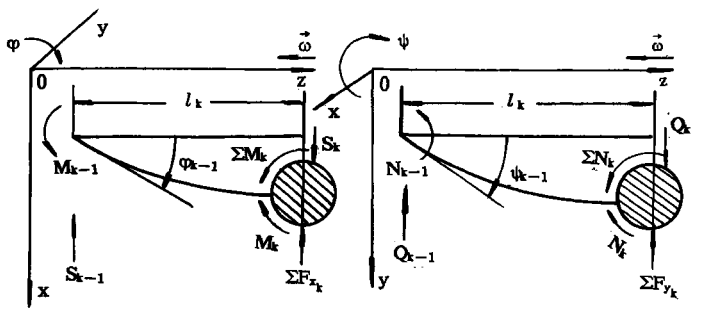

FIGURE 4 Balance of shaft element k.

respectively, W_{x0} and W_{y0} the force components of thrust bearing in x and y directions, and F^j_{x0} and F^j_{y0} the support forces supplied by journal bearing. P_g is the gravity.

As shown in Eqs. (33) and (34), the behaviours of journal and thrust bearings are coupled with the behavior of the rotor. Forces and moments W_{x0}, W_{y0}, M^p_{x0}, and M^p_{y0} involved in Eqs. (33) and (34) are functions of static tilt parameters φ and ψ. Similarly, the supporting forces F^j_{x0} and F^j_{y0} are also functions of the displacements x and y. So solution of Eqs. (33) and (34) needs an iteration procedure.

Offset-Load Effects of Journal Bearings

As the thrust bearing acts on a rotor, support forces supplied by journal bearings must balance not only the gravity of the rotor but also the moments of thrust bearings acting on the xz and yz planes. The components of oil film forces in the x direction is no longer zero. Unfortunately, these static and dynamic characteristics predicted from the vertically loaded case cannot be applied for the offset-loaded case and they must be recalculated except in special cases. When journal bearing under consideration is a 360° journal bearing, let e represents the eccentricity, c the radial clearance, and the eccentricity ratio $\varepsilon = e/c$, the rotordynamic characteristics in an offset-loaded case can be deduced directly from the data obtained in a vertically loaded case (Fig. 5). Let F_{x0} and F_{y0} represent the components of support force of journal bearing in x and y directions under the offset-loaded situation.

$$\begin{aligned} F_{x0} &= W^j \sin a_k \\ F_{y0} &= W^j \cos a_k \end{aligned} \tag{35}$$

where W^j is the load capacity in the vertically loaded case and a_k is the load attitude angle. Assuming isotropic properties, the relationships between the rotordynamic coefficients for the offset-loaded case and that for the vertically loaded case can be expressed as

$$|K_u| = |A_u|\,|K_v|; \quad |D_u| = |A_u|\,|D_v| \tag{36}$$

where $[K_u]$ and $[D_u]$ are, respectively, stiffness and damping coefficient vectors of journal bearing in the offset-loaded case. $[K_v]$ and $[D_v]$ are the stiffness and damping vectors in the vertically loaded case. $[K_u] = (k_{xx'}\ k_{xy'}\ k_{yx'}\ k_{yy'})^T$, $[D_u] = (d_{xx'}\ d_{xy'}\ d_{yx'}\ d_{yy'})^T$, ... The transfer matrix is

$$[A_u] = \begin{bmatrix} \cos^2 a_k & \sin a_k \cos a_k & \sin a_k \cos a_k & \sin^2 a_k \\ -\sin a_k \cos a_k & \cos^2 a_k & -\sin^2 a_k & \sin a_k \cos a_k \\ -\sin a_k \cos a_k & -\sin^2 a_k & \cos^2 a_k & \sin a_k \cos a_k \\ \sin^2 a_k & -\sin a_k \cos a_k & -\sin a_k \cos a_k & \cos^2 a_k \end{bmatrix}. \tag{37}$$

Free Vibration of System

In the case of free vibrations, the moments in Eqs. (31) and (32) become

$$\begin{bmatrix} \Sigma M \\ \Sigma N \end{bmatrix}_k = \begin{bmatrix} M_g \\ N_g \end{bmatrix}_k + \begin{bmatrix} -\Delta M^p_y \\ \Delta M^p_x \end{bmatrix}_k \tag{38}$$

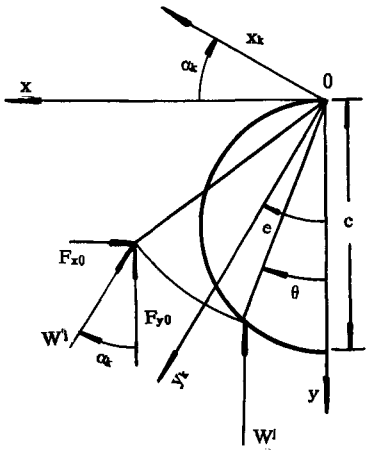

FIGURE 5 Offset-loaded effects of 360° journal bearing.

with the gyroscopic moments

$$\begin{bmatrix} M_g \\ N_g \end{bmatrix}_k = \begin{bmatrix} \theta_y & 0 \\ 0 & \theta_x \end{bmatrix}_k \begin{bmatrix} \ddot{\varphi} \\ \ddot{\psi} \end{bmatrix}_k + \begin{bmatrix} 0 & -\theta_z\omega \\ \theta_z\omega & 0 \end{bmatrix}_k \begin{bmatrix} \dot{\varphi} \\ \dot{\psi} \end{bmatrix}_k \tag{39}$$

and the moments due to thrust bearing can be expressed by using the rotordynamic coefficients.

$$\begin{bmatrix} \Delta M_y^p \\ \Delta M_x^p \end{bmatrix}_k = \begin{bmatrix} k_{y\varphi}^m & k_{y\psi}^m \\ k_{x\varphi}^m & k_{x\psi}^m \end{bmatrix}_k \begin{bmatrix} \varphi \\ \psi \end{bmatrix}_k + \begin{bmatrix} d_{y\varphi}^m & d_{y\psi}^m \\ d_{x\varphi}^m & d_{x\psi}^m \end{bmatrix}_k \begin{bmatrix} \dot{\varphi} \\ \dot{\psi} \end{bmatrix}_k. \tag{40}$$

Forces involved in Eqs. (31) and (32) give

$$\begin{aligned} \begin{bmatrix} \Sigma F_x \\ \Sigma F_y \end{bmatrix}_k &= \begin{bmatrix} m & 0 \\ 0 & m \end{bmatrix}_k \begin{bmatrix} \ddot{x} \\ \ddot{y} \end{bmatrix}_k \\ &+ \begin{bmatrix} k_{xx} & k_{xy} \\ k_{yx} & k_{yy} \end{bmatrix}_k \begin{bmatrix} x \\ y \end{bmatrix}_k + \begin{bmatrix} d_{xx} & d_{xy} \\ d_{yx} & d_{yy} \end{bmatrix}_k \begin{bmatrix} \dot{x} \\ \dot{y} \end{bmatrix}_k \\ &- \begin{bmatrix} k_{x\varphi}^w & k_{x\psi}^w \\ k_{y\varphi}^w & k_{y\psi}^w \end{bmatrix}_k \begin{bmatrix} \varphi \\ \psi \end{bmatrix}_k - \begin{bmatrix} d_{x\varphi}^w & d_{x\psi}^w \\ d_{y\varphi}^w & d_{y\psi}^w \end{bmatrix}_k \begin{bmatrix} \dot{\varphi} \\ \dot{\psi} \end{bmatrix}_k \end{aligned} \tag{41}$$

so the equations of motion for the kth mass point are of the form

$$\begin{bmatrix} m & 0 & 0 & 0 \\ 0 & m & 0 & 0 \\ 0 & 0 & \theta_y & 0 \\ 0 & 0 & 0 & \theta_x \end{bmatrix}_k \begin{bmatrix} \ddot{x} \\ \ddot{y} \\ \ddot{\varphi} \\ \ddot{\psi} \end{bmatrix}_k +$$

$$\begin{bmatrix} d_{xx} & d_{xy} & -d_{x\varphi}^w & -d_{x\psi}^w \\ d_{yx} & d_{yy} & -d_{y\varphi}^w & -d_{y\psi}^w \\ 0 & 0 & -d_{y\varphi}^m & -d_{y\psi}^m - \theta_z\omega \\ 0 & 0 & \theta_z\omega + d_{x\varphi}^m & d_{x\psi}^m \end{bmatrix}_k \begin{bmatrix} \dot{x} \\ \dot{y} \\ \dot{\varphi} \\ \dot{\psi} \end{bmatrix}_k$$

$$+ \begin{bmatrix} k_{xx} & k_{xy} & -k_{x\varphi}^w & -k_{x\psi}^w \\ k_{yx} & k_{yy} & -k_{y\varphi}^w & -k_{y\psi}^w \\ 0 & 0 & -k_{y\varphi}^m & -k_{y\psi}^m \\ 0 & 0 & k_{x\varphi}^m & k_{x\psi}^m \end{bmatrix}_k \begin{bmatrix} x \\ y \\ \varphi \\ \psi \end{bmatrix}_k$$

$$- \begin{bmatrix} \frac{12EI}{l^3} & 0 & \frac{-6EI}{l^2} & 0 \\ 0 & \frac{12EI}{l^3} & 0 & \frac{-6EI}{l^2} \\ \frac{6EI}{l^2} & 0 & \frac{-2EI}{l} & 0 \\ 0 & \frac{6EI}{l^2} & 0 & \frac{-2EI}{l} \end{bmatrix}_{k+1} \begin{bmatrix} x \\ y \\ \varphi \\ \psi \end{bmatrix}_{k+1}$$

$$- \begin{bmatrix} \frac{12EI}{l^3} & 0 & \frac{6EI}{l^2} & 0 \\ 0 & \frac{12EI}{l^3} & 0 & \frac{6EI}{l^2} \\ \frac{-6EI}{l^2} & 0 & \frac{-2EI}{l} & 0 \\ 0 & \frac{-6EI}{l^2} & 0 & \frac{-2EI}{l} \end{bmatrix}_k \begin{bmatrix} x \\ y \\ \varphi \\ \psi \end{bmatrix}_{k-1}$$

$$+ \begin{bmatrix} \frac{12EI}{l^3} & 0 & \frac{6EI}{l^2} & 0 \\ 0 & \frac{12EI}{l^3} & 0 & \frac{6EI}{l^2} \\ \frac{6EI}{l^2} & 0 & \frac{4EI}{l} & 0 \\ 0 & \frac{6EI}{l^2} & 0 & \frac{4EI}{l} \end{bmatrix}_{k+1} \begin{bmatrix} x \\ y \\ \varphi \\ \psi \end{bmatrix}_k$$

$$+ \begin{bmatrix} \frac{12EI}{l^3} & 0 & \frac{-6EI}{l^2} & 0 \\ 0 & \frac{12EI}{l^3} & 0 & \frac{-6EI}{l^2} \\ \frac{-6EI}{l^2} & 0 & \frac{4EI}{l} & 0 \\ 0 & \frac{-6EI}{l^2} & 0 & \frac{4EI}{l} \end{bmatrix}_k \begin{bmatrix} x \\ y \\ \varphi \\ \psi \end{bmatrix}_k = 0. \tag{42}$$

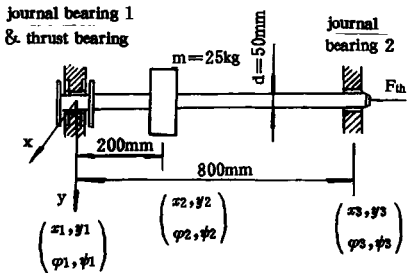

FIGURE 6 Rotor system equipped with journal and thrust bearings.

When applying Eq. (42) to all mass points, we have the system equation in matrix form given by

$$[M][\ddot{x}] + [C][\dot{x}] + [K]x] = 0 \qquad (43)$$

where $[M]$, $[C]$, and [K] are the mass, damping, and stiffness matrixes, respectively, and $[x]$ is the displacement vector.

EXAMPLE AND DISCUSSION

A rotor system shown in Fig. 6 is used to verify the theoretical analysis. The rotor is supported by a 360° journal bearing at the right end and a combined journal and thrust bearing at the left end. The combined journal and thrust bearing consists of a 360° journal bearing and two fixed eight-pad thrust bearings on either side with identical parameters. Parameters of the rotor are also shown in Fig. 6. Two 360° journal bearings have the same parameters with the diameter $D_0 = 50$ mm, the length of journal bearing $L = 25$ mm, the radial clearance $c = 0.025$ mm and the clearance ratio $\Psi = (2c/D_0) = 0.001$.

Each thrust bearing consists of eight pads evenly distributed in the circumferential direction with pad parameters: $r_1 = 25$ *mm*, $B = 50$ *mm*, $\theta = 40°$, $\alpha_0 = 0.002$, $\theta_p = \theta_0/2$, $h_e/B = 0.001$, and the total axial clearance $2h_e = 0.1$ mm. The dynamic viscosity of the oil, $\mu = 0.02706\ Ns/m^2$.

The external axial thrust acting at the right end of the rotor is $F_{th} = 0.0$. Because there is no external axial thrust axial thrust acting on the rotor, components of forces produced by two thrust bearings are self-balanced in the x, y, and z directions. Besides the gravity of the rotor and the support forces of the journal bearings, the rotor is subjected to the moments of the thrust bearings in the static balance state. In the present study, performances of the thrust bearing are calculated by the out-domain method, and the theoretical solutions, which are based on the short bearing theory in Pinkus and Sternlicht (1961), are adopted to find the characteristics of 360° journal bearing for the vertically loaded case, and Eqs. (35–37) are used to take into account the offset-loaded effect.

A generalized inverse iteration method described in Zheng et al. (1989) is used to solve the quadratic eigenvalue problem (43). Numerical results include the characteristics of journal and thrust bearings, the deflection curves, the load distributions, and the eigenvalues of the system for a range of rotating speeds from $N = 3000$ rpm to $N = 9064$ rpm.

Influence of φ_0 and ψ_0 on Thrust Bearing Performance. In Table 1 are listed the static moments and the dynamic coefficients with various $\bar{\varphi}_0$ and $\bar{\psi}_0$. The importance of the static tilt of the runner is obviously shown. Taking the data with $\bar{\varphi}_0 = 0$ and $\bar{\psi}_0 = 0$ as standard, in the case of $\bar{\varphi}_0 = 0.4$ and $\bar{\psi}_0 = 0.2$, the dimensionless moment stiffness coefficient $\bar{k}^m_{x\varphi}$ is about 3.3 times as large as the value with $\bar{\varphi}_0$ and $\bar{\psi}_0 = 0$. Similar conclusions can be obtained for the discussion on other parameters. So the tilt parameters change thrust bearing performance greatly.

Table 1. Effects of Tilt Parameters on Thrust Bearing Performance

	$\bar{M}^p_{y0}$	$\bar{M}^p_{x0}$	$\bar{k}^m_{x\varphi}$	$\bar{k}^m_{x\psi}$	$\bar{d}^m_{x\varphi}$	$\bar{d}^m_{x\psi}$	$\bar{k}^m_{y\varphi}$	$\bar{k}^m_{y\psi}$	$\bar{d}^m_{y\varphi}$	$\bar{d}^m_{y\psi}$
$\bar{\varphi} = 0$, $\bar{\psi} = 0$	0.0	0.0	0.094	0.388	0.001	0.19	−0.388	0.094	−0.190	0.001
$\bar{\varphi} = 0.1$, $\bar{\psi} = 0.1$	0.049	−0.03	0.109	0.413	0.004	0.196	−0.410	0.085	−0.196	−0.002
$\bar{\varphi} = 0.4$, $\bar{\psi} = 0.2$	0.152	−0.194	0.311	0.638	0.036	0.242	−0.851	−0.047	−0.295	−0.033

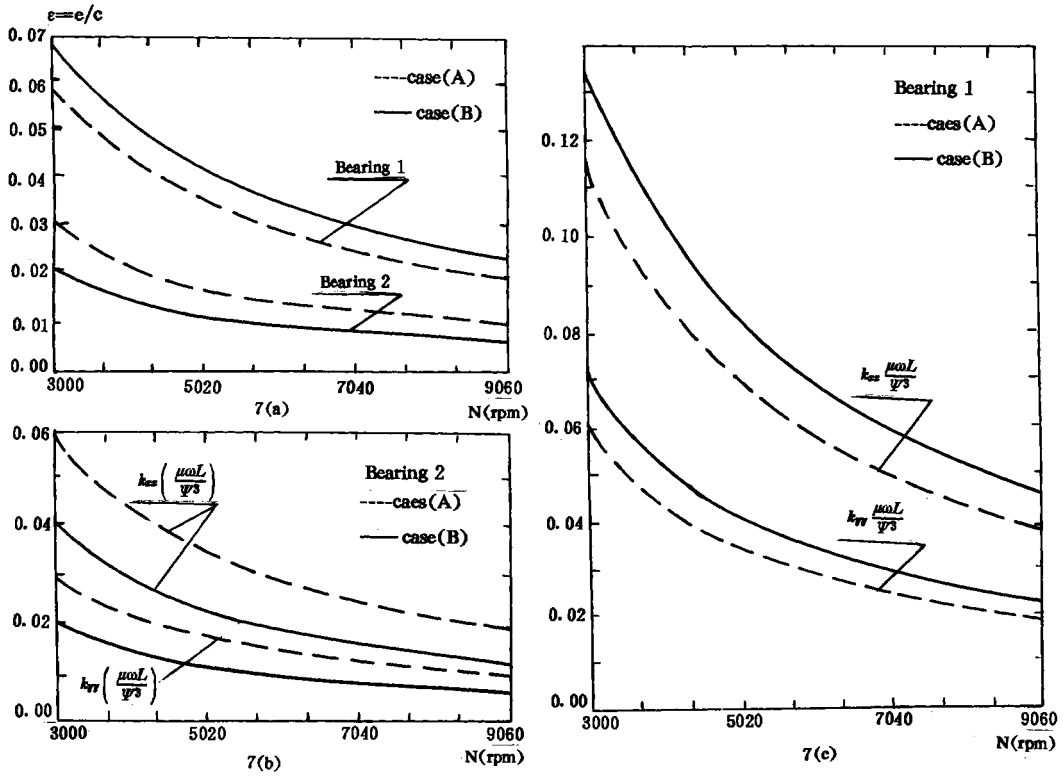

FIGURE 7 (a) Eccentricity ratio curves versus rotating speed and (b), (c) variation of stiffness coefficients due to offset-loaded effects of journal bearings.

Effects of Thrust Bearing on Journal Bearings. Figure 7(a) shows the variation of eccentricity ratio ε of journal bearings versus varied rotating speed. In this example, thrust bearings lead to an increase in eccentricity of journal bearing 1, and a decrease in that of journal bearing 2 at a certain speed. Effects of thrust bearings on the rotordynamic coefficients of two journal bearings are illustrated in Figs. 7(b, c). Taking $N = 9064$ rpm as an example, when the effects of thrust bearing are considered (case B), ε_1, $k_{xx}^{(1)}$, $k_{yy}^{(1)}$ all increase nearly by a factor of 20% compared with the values while considering journal bearings alone (case A). For the second journal bearing, ε_2, $k_{xx}^{(2)}$, and $k_{yy}^{(2)}$ decrease by a factor of 32–37% because of the action of the thrust bearings.

Static Deflection of Rotor. In Table 2, case C represents the rotor with rigid support, and case B represents the rotor with journal and thrust bearings attached. Three sets of data of deflection of the rotor are given. Because M_{x0}^{p} and M_{y0}^{p} are all functions of rotating speed, it follows that parameters $x_1, y_1, \ldots, \varphi_3$, and ψ_3 are all varied with N. Generally, with increased N, M_{x0}^{p} and M_{y0}^{p} make the static deflection of the rotor decrease. Taking $N = 9064$ rpm as an example, static deflection y_2 at the mass center decreases

Table 2. Static Deflection of Rotor

Case	y_1/D_0	y_2/D_0	y_3/D_0	ψ_1	ψ_2	ψ_3
C	0.0	0.56×10^{-3}	0.0	0.16×10^{-3}	0.93×10^{-4}	-0.12×10^{-3}
B (n = 3000 rpm)	0.31×10^{-5}	0.23×10^{-3}	-0.39×10^{-7}	0.36×10^{-4}	0.49×10^{-4}	-0.53×10^{-4}
B (n = 9046 rpm)	0.38×10^{-6}	0.17×10^{-3}	-0.20×10^{-7}	0.14×10^{-4}	0.42×10^{-4}	-0.42×10^{-4}

Table 3. Logarithmic Attenuation Ratio of Eigenvalue γ_1

N(rpm)	3000	5010	7020	9030	10,000	13,000	14,000
U_1/ω (case A)	0.027	0.015	0.010	0.003	−0.006	—	—
U_1/ω (case B)	0.019	0.011	0.007	0.005	0.004	0.001	−0.002

with a factor of 70% when compared to the value in the case of the rigid support. Thrust bearings change the static deflection of the rotor to a great extent because of their constraining effects.

System Stability. In order to analyze system stability, eigenvalues of the system are found by solving Eq. (43). The results show that the first damped critical speed of the system is $N_{cr} = 5653$ rpm when considering journal bearings alone, and the first damped critical speed is $N_{cr}^* = 10445$ rpm when both journal and thrust bearings are considered. It can be seen that N_{cr}^* is nearly 1.85 times as large as N_{cr}. Thrust bearings lead to a considerable increase in the damped critical speed of the system. As to the system stability, the results show that thrust bearings have little influence on the whirl frequency of the first eigenvalue $\gamma_1(\gamma_1 = -U_1 + iV_1)$, the whirl ratio (V_1/ω) is close to 0.5 and remains almost unchanged. This may be because the journal bearings operate with a small eccentricity in the present case. On the other hand, action of thrust bearings changes the logarithmic attenuation ratio U_1/ω. The logarithmic attenuation ratios are listed in Table 3.

The threshold speed of stability of the system is about 9400 rpm when the rotor is supported by journal bearings alone (case A); while the same system remains stable until N reaches 13220 rpm after the rotor is equipped with thrust bearings (case B), which is about 1.41 times larger than the value in case A. Action of the thrust bearing delays the instability of the system considerably.

CONCLUSIONS

Rotordynamic coefficients of thrust bearing were introduced and calculated by using the out-domain method. A general analysis method, in which the coupling action among the rotor, the journal, and thrust bearings is taken into account, was developed. The effects of the thrust bearing were shown in many respects such as the load redistribution and the offset-loaded effects, especially in the static deflection of the rotor, the damped critical speed, and the system stability. It must be pointed out that in the present research, although the fixed-pad thrust bearings are considered only, similar analysis can be applied to pivoted-pad thrust bearing and was omitted here for brevity. So it is necessary to consider the effects of thrust bearing on system dynamics when a rotor is equipped with journal and thrust bearing simultaneously.

APPENDIX A

In Eq. (4), $\nabla^2 U_s = f_s + g_s U_s$, the coefficients give

$$g_s = \frac{3}{4} a^{-2}\left[\left(\frac{\partial a}{\partial \bar{x}}\right)^2 + \left(\frac{\partial a}{\partial \bar{y}}\right)^2\right] + \frac{3}{2} a^{-1}\left[\frac{\partial^2 a}{\partial \bar{x}^2} + \frac{\partial^2 a}{\partial \bar{y}^2}\right]$$

$$f_s = \begin{cases} 6a^{-3/2}\dfrac{\partial a}{\partial \theta}\bar{\mu}^{1/3} & (\text{for } s = 0) \\ -\dfrac{3}{2}\bar{\mu}^{-1/3}a^{-2}\left\{a^{-1}\left[\left(\dfrac{\partial a}{\partial \bar{x}}\right)^2 + \left(\dfrac{\partial a}{\partial \bar{y}}\right)^2\right] + \left[\dfrac{\partial^2 a}{\partial \bar{x}^2} + \dfrac{\partial^2 a}{\partial \bar{y}^2}\right]\right\} U_0 - 9a^{-5/2}\dfrac{\partial a}{\partial \theta} & (\text{for } s = z) \\ \dfrac{3}{2}\bar{\mu}^{-1/3}a^{-2}\left\{\bar{r}\sin\theta a^{-1}\left[\left(\dfrac{\partial a}{\partial \bar{x}}\right)^2 + \left(\dfrac{\partial a}{\partial \bar{y}}\right)^2\right] - \dfrac{\partial a}{\partial \bar{x}} + \bar{r}\sin\theta\left(\dfrac{\partial^2 a}{\partial \bar{x}^2} + \dfrac{\partial^2 a}{\partial \bar{y}^2}\right)\right\} U_0 + 6\bar{r}a^{-3/2}\left[\dfrac{3}{2}a^{-1}\sin\theta\dfrac{\partial a}{\partial \theta} - \cos\theta\right] & (\text{for } s = \varphi) \\ \dfrac{3}{2}\bar{\mu}^{-1/3}a^{-2}\left\{\bar{r}\cos\theta a^{-1}\left[\left(\dfrac{\partial a}{\partial \bar{x}}\right)^2 + \left(\dfrac{\partial a}{\partial \bar{y}}\right)^2\right] - e\dfrac{\partial a}{\partial \bar{y}} + \bar{r}\cos\theta\left(\dfrac{\partial^2 a}{\partial \bar{x}^2} + \dfrac{\partial^2 a}{\partial \bar{y}^2}\right)\right\} U_0 + 6\bar{r}a^{-3/2}\left[\dfrac{3}{2}a^{-1}\cos\theta\dfrac{\partial a}{\partial \theta} + \sin\theta\right] & (\text{for } s = \psi) \\ 12a^{-3/2} & (\text{for } s = z') \\ -12a^{-3/2}\bar{r}\sin\theta & (\text{for } s = \varphi') \\ -12a^{-3/2}\bar{r}\cos\theta & (\text{for } s = \psi'). \end{cases}$$

APPENDIX B

Definition of dimensionless rotordynamic coefficients:

$$\bar{k}^W_{zz} = k^W_{zz}\left(\frac{h_e^3}{\mu_0\omega B^4}\right) = \int\int_\Omega \frac{\partial P}{\partial \bar{z}}\,\bar{r}\,d\bar{r}\,d\theta$$

$$\bar{k}^W_{z\varphi} = k^W_{z\varphi}\left(\frac{h_e^3}{\mu_0\omega B^5}\right) = \int\int_\Omega \frac{\partial P}{\partial \bar{\varphi}}\,\bar{r}\,d\bar{r}\,d\theta$$

$$\bar{k}^W_{z\psi} = k^W_{z\psi}\left(\frac{h_e^3}{\mu_0\omega B^5}\right) = \int\int_\Omega \frac{\partial P}{\partial \bar{\psi}}\,\bar{r}\,d\bar{r}\,d\theta$$

$$\bar{d}^W_{zz} = d^W_{zz}\left(\frac{h_e^3}{\mu_0 B^4}\right) = \int\int_\Omega \frac{\partial P}{\partial \bar{z}'}\,\bar{r}\,d\bar{r}\,d\theta$$

$$\bar{d}^W_{z\varphi} = d^W_{z\varphi}\left(\frac{h_e^3}{\mu_0 B^5}\right) = \int\int_\Omega \frac{\partial P}{\partial \bar{\varphi}'}\,\bar{r}\,d\bar{r}\,d\theta$$

$$\bar{d}^W_{z\psi} = d^W_{z\psi}\left(\frac{h_e^3}{\mu_0 B^5}\right) = \int\int_\Omega \frac{\partial P}{\partial \bar{\psi}'}\,\bar{r}\,d\bar{r}\,d\theta$$

$$\begin{vmatrix} k^W_{xz} \\ k^W_{x\varphi} \\ k^W_{x\psi} \end{vmatrix} = \begin{vmatrix} \varphi_0 k^W_{zz} \\ \varphi_0 k^W_{z\varphi} + W_0 \\ \varphi_0 k^W_{z\psi} \end{vmatrix} \quad \begin{vmatrix} d^W_{xz} \\ d^W_{x\varphi} \\ d^W_{x\psi} \end{vmatrix} = \varphi_0 \begin{vmatrix} d^W_{zz} \\ d^W_{z\varphi} \\ d^W_{z\psi} \end{vmatrix}$$

$$\begin{vmatrix} k^W_{yz} \\ k^W_{y\varphi} \\ k^W_{y\psi} \end{vmatrix} = \begin{vmatrix} \psi_0 k^W_{zz} \\ \psi_0 k^W_{z\varphi} \\ \psi_0 k^W_{z\psi} + W_0 \end{vmatrix} \quad \begin{vmatrix} d^W_{yz} \\ d^W_{y\varphi} \\ d^W_{y\psi} \end{vmatrix} = \psi_0 \begin{vmatrix} d^W_{zz} \\ d^W_{z\varphi} \\ d^W_{z\psi} \end{vmatrix}$$

$$\bar{k}^m_{xz} = k^m_{xz}\left(\frac{h_e^3}{\mu_0\omega B^5}\right) = \int\int \frac{\partial P}{\partial \bar{z}}\,\bar{r}^2\cos\theta\,d\bar{r}\,d\theta$$

$$\bar{k}^m_{x\varphi} = k^m_{x\varphi}\left(\frac{h_e^3}{\mu_0\omega B^6}\right) = \int\int \frac{\partial P}{\partial \bar{\varphi}}\,\bar{r}^2\cos\theta\,d\bar{r}\,d\theta$$

$$\bar{k}^m_{x\psi} = k^m_{x\psi}\left(\frac{h_e^3}{\mu_0\omega B^6}\right) = \int\int \frac{\partial P}{\partial \bar{\psi}}\,\bar{r}^2\cos\theta\,d\bar{r}\,d\theta$$

$$\bar{d}^m_{xz} = d^m_{xz}\left(\frac{h_e^3}{\mu_0 B^5}\right) = \int\int \frac{\partial P}{\partial \bar{z}'}\,\bar{r}^2\cos\theta\,d\bar{r}\,d\theta$$

$$\bar{d}^m_{x\varphi} = d^m_{x\varphi}\left(\frac{h_e^3}{\mu_0 B^6}\right) = \int\int \frac{\partial P}{\partial \bar{\varphi}'}\,\bar{r}^2\cos\theta\,d\bar{r}\,d\theta$$

$$\bar{d}^m_{x\psi} = d^m_{x\psi}\left(\frac{h_e^3}{\mu_0 B^6}\right) = \int\int \frac{\partial P}{\partial \bar{\psi}'}\,\bar{r}^2\cos\theta\,d\bar{r}\,d\theta$$

$$\bar{k}^m_{yz} = k^m_{yz}\left(\frac{h_e^3}{\mu_0\omega B^5}\right) = \int\int_\Omega -\frac{\partial P}{\partial \bar{z}}\,\bar{r}^2\sin\theta\,d\bar{r}\,d\theta$$

$$\bar{k}^m_{y\varphi} = k^m_{y\varphi}\left(\frac{h_e^3}{\mu_0\omega B^6}\right) = \int\int_\Omega -\frac{\partial P}{\partial \bar{\varphi}}\,\bar{r}^2\sin\theta\,d\bar{r}\,d\theta$$

$$\bar{k}^m_{y\psi} = k^m_{y\psi}\left(\frac{h_e^3}{\mu_0\omega B^6}\right) = \int\int_\Omega -\frac{\partial P}{\partial \bar{\psi}}\,\bar{r}^2\sin\theta\,d\bar{r}\,d\theta$$

$$\bar{d}^m_{yz} = d^m_{yz}\left(\frac{h_e^3}{\mu_0 B^5}\right) = \int\int_\Omega -\frac{\partial P}{\partial \bar{z}'}\,\bar{r}^2\sin\theta\,d\bar{r}\,d\theta$$

$$\bar{d}^m_{y\varphi} = d^m_{y\varphi}\left(\frac{h_e^3}{\mu_0 B^6}\right) = \int\int_\Omega -\frac{\partial P}{\partial \bar{\varphi}'}\,\bar{r}^2\sin\theta\,d\bar{r}\,d\theta$$

$$\bar{d}^m_{y\psi} = d^m_{y\psi}\left(\frac{h_e^3}{\mu_0 B^6}\right) = \int\int_\Omega -\frac{\partial P}{\partial \bar{\psi}'}\,\bar{r}^2\sin\theta\,d\bar{r}\,d\theta$$

$$\begin{vmatrix} k^m_{zz} \\ k^m_{z\varphi} \\ k^m_{z\psi} \end{vmatrix} = \begin{vmatrix} -(\varphi_0 k^m_{xz} + \psi_0 k^m_{yz}) \\ -(\varphi_0 k^m_{x\varphi} + \psi_0 k^m_{y\varphi} + M_{x0}) \\ -(\varphi_0 k^m_{x\psi} + \psi_0 k^m_{y\psi} + M_{y0}) \end{vmatrix} \quad \begin{vmatrix} d^m_{zz} \\ d^m_{z\varphi} \\ d^m_{z\psi} \end{vmatrix} = \begin{vmatrix} -(\varphi_0 d^m_{xz} + \psi_0 d^m_{yz}) \\ -(\varphi_0 d^m_{x\varphi} + \psi_0 d^m_{y\varphi}) \\ -(\varphi_0 d^m_{x\psi} + \psi_0 d^m_{y\psi}) \end{vmatrix}$$

REFERENCES

Etsion, I., 1978, "Design Charts for Arbitrarily Pivoted, Liquid-Lubricated, Flat-Sector-Pad Thrust Bearing," *Journal of Lubrication Technology, Trans. ASME,* Vol. 100, pp. 279–286.

Jeng, M. C., and Szeri, A. Z., 1986, "A Thermohydrodynamic Solution of Pivoted Thrust Pads," *Journal of Tribology, Trans. ASME,* Vol. 108, pp. 195–218.

Mittwollen, N., Hegel, T., and Glienicke, J., 1990, "Effects of Hydrodynamic Thrust Bearings on Lateral Shaft Vibration," *Journal of Tribology, Trans. ASME,* Vol. 113, pp. 811–818.

Myklestad, N. O., 1944, "A New Method for Calculating Natural Modes of Uncoupled Bending Vibration of Airplane Wings and Other Types of Beams," *Journal of Aerospace Science,* Vol. 11, pp. 153–162.

Patterson, C., and Sheikh, M. A., 1982, "On the Use of Fundamental Solution in Trefftz Method of Potential and Elasticity Problems," in C. A. Brebbia, *Boundary Element Method in Engineering,* Computational Mechanics Centre Publication.

Pinkus, O., and Sternlicht, B., 1961, *Theory of Hydrodynamic Lubrication,* McGraw-Hill Book Company, Inc., New York, p. 54.

Someya, T., and Fukuda, M., 1972, "Analysis and Experimental Verification of Dynamic Characteristics of Oil Film Thrust Bearings," *Bulletin of JSME,* Vol. 15, pp. 1004–1015.

Trefftz, E., 1926, "Ein Gegenstruck zum Ribzschem Verfharen," *Proceedings of the 2nd International Congress of Applied Mechanics,* Zurich.

T. S. Zheng, et al., 1989, "A Generalized Inverse Iteration Method for Solution of Quadratic Eigenvalue Problems in Structural Dynamic Analysis," *Computers and Structures,* Vol. 33, pp. 1139–1143.

Qin, Zhu, You-Bai, Xie, Lie, Yu, 1990, "Axial Transient Forces of Thrust Bearing Rotor System in a Turboexpander," *Proceedings of the International Conference on Hydrodynamic Bearing-Rotor System Dynamics,* China.